Int. J. Electrochem. Sci., 7 **(2012)** 4596 - 4607

International Journal of
ELECTROCHEMICAL
SCIENCE
www.electrochemsci.org

Production, Physicochemical Characterization and Magnetic Behavior of Nanocrystalline Al- Doped Co/Fe System

N. M. Deraz[*]

Chemistry Department, College of Science, King Saud University, Riyadh, Saudi Arabia
[*]E-mail: nmderaz@yahoo.com

Received: 27 March 2012 / *Accepted:* 19 April 2012 / *Published:* 1 May 2012

Nanocrystalline cobalt ferrite with a nominal composition of $CoFe_2O_4$ was prepared by combustion synthesis. The influence of alumina-doping on the physicochemical and magnetic properties of $CoFe_2O_4$ nano-particles were investigated by means of X-ray powder diffraction (XRD), infrared (IR) spectroscopy, scanning electron microscopy (SEM) and vibrating sample magnetometer (VSM). XRD and IR analyses confirm that the doping with 3 wt % alumina resulted in the formation of cubic spinel phase of $CoFe_2O_4$ nano-particles. Undpoed and alumina doped cobalt ferrite presented in a uniform microstructure with grain size in nano-scale. Alumina treatment led to a decrease in the coercivity(H_c) and an increase in both magnetization (M_s) and magnetic moment (n_B) of the investigated system. The maximum increase in the values of both M_s and n_B due to the treatment with 3 wt% alumina attained 29.8 %. The observed results can be explained on the basis of particle size and the Fe^{3+} concentration in the octahedral and tetrahedral sites involved in the cubic spinel structure.

Keywords: XRD; IR; SEM; M_s; alumina-doped $CoFe_2O_4$

1. INTRODUCTION

Iron and cobalt mixed oxides undergo solid state reaction to produce cobalt ferrite that appears as film to cover the grains of each reacting oxide. So, the propagation of this reaction is controlled by thermal diffusion of cobalt and iron cations through the ferrite film which acts as an energy barrier. The rate of diffusion and reactivity can be increased by raising the preparation temperature, forming a more reactive precursor, presence of impurities and effectiveness of phase boundary contacts [1]. Various successful attempts have been done to simulate the ferrites formation via doping with certain foreign oxides [1- 5]. In fact, it has been reported that Al_2O_3 –doping enhanced the formation of manganese and zinc ferrites [2, 3]. However, ZnO and Li_2O being added as dopants stimulated the formation of Mn and Cu ferrites, repectively [1, 4]. The enhancement of ferrites formation due to

doping had been attributed to an effective increase in the mobility of reacting cations taking part in the ferrite formation.

Nanocrystalline magnetic cobalt ferrite is gaining attraction due to many important applications such as ferrofluids, magnetic drug delivery and hyperthermia for cancer treatment [6]. The remarkable properties of cobalt ferrite such as moderate saturation magnetization, high coercivity, strong anisotropy along with good mechanical hardness and chemical stability are not observed in the bulk sample [7]. These properties, along with their great physical and chemical stability, resulted in different technological applications of this ferrite. Cobalt ferrite is ordinarily an almost inverse cubic spinel in which the degree of inversion is critically determined by the preparation conditions [8]. In addition, Co^{2+} cations can be migrating from octahedral (B-sublattice) to tetrahedral places (A-sublattice). So, it can be suggested that the spinel structure in the prepared materials having the formula $CoFe_2O_4$ and can be expressed as:

$$(Fe_{1-x}{}^{3+}\ Co_x{}^{2+})_A[Co_{1-x}{}^{2+}\ Fe_{1+x}{}^{3+}]_B\ O_4{}^{2-}$$

where the parameter of inversion, x, is greater than 0 and smaller than 1. In cubic spinel structured $CoFe_2O_4$ system, the O^{2-} ions form fcc close packing, and the Co^{2+} and Fe^{3+} occupy either tetrahedral or octahedral interstitial sites [9]. These two antiparallel sublattices, which are coupled by superexchange interactions through the O^{2-} ions, form the ferrimagnetic structure.

Preparation of nanomaterials with accurately controlled particle size, narrow size distribution and low-degree agglomeration is still a big challenge. Recently, different synthetic routes to prepare highly crystalline and uniformly sized magnetic nanoparticles of cobalt ferrite have been reported [10–13]. These methods require expensive and often toxic reagents, complicated synthetic steps, high reaction temperature and long reaction time. So, most of these methods cannot be applied to a large scale and economic production. Among the current methods for synthesis of cobalt ferrite, the combustion route is an alternative and highly promising method for the synthesis of this ferrite [14, 15]. This method is quite simple, fast, and inexpensive and also is easy to control in the stoichiometry and crystallite size which have influence on the magnetic properties of the ferrite. The basis of this route comes from the thermochemical concepts used in propellant chemistry and explosives [16]. Indeed, this method displays an exothermic, very rapid and self-sustaining chemical reaction between the desired metal salts and a suitable organic fuel. Consequently, a key feature of this method is that the heat required to occur the chemical reaction is provided by the reaction itself and not by an external source [16, 17].

Magnetic nanoparticles of undoped cobalt ferrite have been synthesized by combustion route employing glycine or a mixture of glycine and ammonium nitrate as fuel with the corresponding metal nitrates [8].When glycine alone is used as fuel, nano-sized $CoFe_2O_4$ phase is formed with CoO being in the moderate crystalline state. When the mixture of glycine and ammonium nitrate is used, well-crystalline $CoFe_2O_4$ is obtained as a single phase. The saturation magnetization (M_s), remnant magnetization (M_r) and coercivity were found to be highly in presence of a mixture of glycine and ammonium nitrate depending upon the size and crystallinity of the investigated ferrite.

It is well-known that when ferrites are sufficiently diluted with non-magnetic atoms, they can show a wide spectrum of magnetic structures, ferrimagnetic order, cluster spin glass etc. [18]. Effects addition of aluminum or titanium on the magnetic properties of cobalt ferrite synthesized by sol–gel method has been studied. It reported that the coercivity is less while saturation magnetization is more in $Al_{0.2}CoFe_{1.8}O_4$ (870 Oe and 72.1 emu/g), in respect of $Ti_{0.2}Co_{1.2}Fe_{1.6}O_4$ (1.56 kOe and 62.6 emu/g)[19]. However, The unit cell parameter and saturation magnetization of alumina substituted cobalt prepared by aerosol route, decrease linearly with the increase of alumina concentration. This is due to the smaller ionic radius and the diamagnetic nature of aluminum ion [20].

The present work is focused on the effects of alumina-doping on the structural, morphological and magnetic properties of cobalt ferrite obtained via combustion route. The X-ray powder diffraction patterns, the microstructure and the magnetic properties are discussed as a function of the dopant content.

2. EXPERIMENTAL

2.1. Materials

Three samples of alumina-doped $CoFe_2O_4$ system were prepared by mixing calculated proportions of cobalt and iron nitrates with glycine as fuel and different amounts of aluminum nitrate. The mixed precursors were concentrated in a porcelain crucible on a hot plate at 350 ^oC for 10 minutes. The crystal water was gradually vaporized during heating and when a crucible temperature was reached, a great deal of foams produced and spark appeared at one corner which spread through the mass, yielding a voluminous and fluffy product in the container. In our experiments, the ratio of the mixture glycine: cobalt and ferric nitrates was 1.33. The concentrations of aluminum expressed as wt% Al_2O_3 were 1.5 and 3. The chemicals employed in the present work were of analytical grade supplied by Prolabo Company.

2.2. Techniques

An X-ray measurement of various mixed solids was carried out using a BRUKER D8 advance diffractometer. The patterns were run with Cu K_α radiation at 40 kV and 40 mA with scanning speed in 2θ of 2 ° min^{-1}.

The crystallite size of undoped and alumina doped cobalt ferrite present in the investigated solids was based on X-ray diffraction line broadening and calculated from the most intense plane (311) using Scherrer equation [21].

$$d = \frac{B\lambda}{\beta \cos\theta} \qquad (1)$$

where d is the average crystallite size of the phase under investigation, B is the Scherrer constant (0.89), λ is the wave length of X-ray beam used, β is the full-with half maximum (FWHM) of diffraction and θ is the Bragg's angle.

An infrared transmission spectrum of various solids was determined using Perkin-Elmer Spectrophotometer (type 1430). The IR spectra were determined from 1000 to 350 cm^{-1}. Two mg of each solid sample were mixed with 200 mg of vacuum-dried IR-grade KBr. The mixture was dispersed by grinding for 3 min in a vibratory ball mill and placed in a steel die 13 mm in diameter and subjected to a pressure of 12 tonnes. The sample disks were placed in the holder of the double grating IR spectrometer.

Scanning electron micrographs (SEM) were recorded on JEOL JAX-840A and JEOL JEM-1230 electron micro-analyzers, respectively. The samples were dispersed in ethanol and then treated ultrasonically in order disperse individual particles over a gold grids.

The magnetic properties of the investigated solids were measured at room temperature using a vibrating sample magnetometer (VSM; 9600-1 LDJ, USA) in a maximum applied field of 15 kOe. From the obtained hysteresis loops, the saturation magnetization (M_s), remanence magnetization (M_r) and coercivity (H_c) were determined.

3. RESULTS AND DISCUSSION

3.1. XRD analysis

The X-ray diffractograms of undoped and alumina doped $CoFe_2O_4$ nano-particles fabricated by the combustion technique are depicted in Fig. 1.

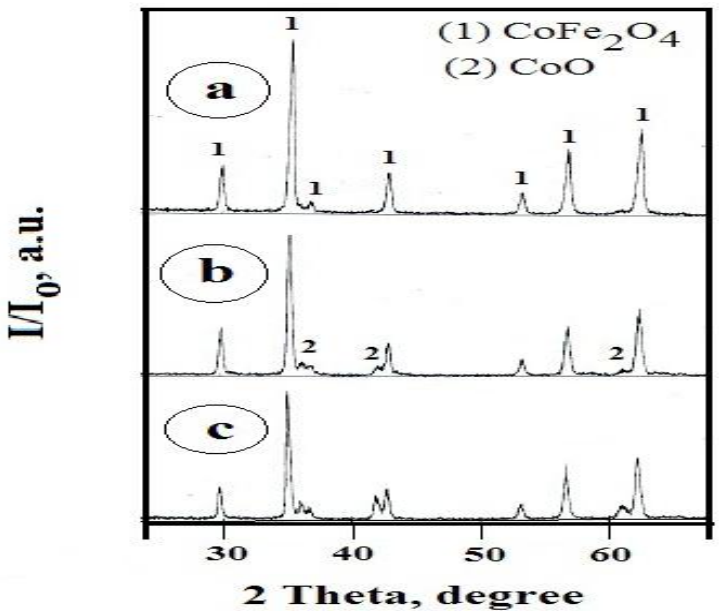

Figure 1. X-ray diffraction patterns of $CoFe_2O_4$ sample treated with different amounts of aluminum oxide; (a) 0 wt% Al_2O_3, (b) 1.5 wt% Al_2O_3 and (c) 3 wt% Al_2O_3.

All the characteristic peaks of spinel $CoFe_2O_4$ phase are present in the investigated diffractograms. Obvious trace amounts of CoO as a second phase can be detected in the pure and 1.5 wt% alumina doped samples. However, a sharp increase in the crystallinity of the cobalt ferrite powders is observed as the amount of aluminum oxide was increased, which is recorded as a decrease in the broadening of the peaks in the diffraction patterns. Indeed, alumina doping brought about an increase in the peak height of cobalt ferrite phase with subsequent a decrease in those of CoO phase. In addition, doping of the investigated system with 3 wt% alumina led to completely disappearance of all peaks related to CoO phase with formation of single phase of cobalt ferrite. This finding indicates complete conversion of Co and Fe oxides to $CoFe_2O_4$ crystallites suggesting an increase in the amount of desired ferrite. In other words, Al_2O_3 doping supplies larger motion force for the formation of the ferrite phase with larger crystallinity via the conversion of un-reacted oxides with subsequent increase the number of Fe^{3+} ions involved in the spinel structure via converting Fe^{2+} ions that may be present in Fe_2O_3 crystals [3].

The promotion effect of Al_2O_3- doping in the formation of cubic spinel structure of cobalt ferrite due to the alumina-doping could result from an induced increase in the concentration of the reacting species and/or increasing their mobility. The induced increase in the mobility of Co^{2+} and Fe^{3+} ions could be attributed to the introduction of Al^{3+} ions in the as prepared lattices. This occurs due to the ionic radius input difference of these ions. In fact, the ionic radius of the Al^{3+} ion is 0.050 nm, while the ionic radii of the Co^{2+}, Fe^{2+} and Fe^{3+} ions 0.078, 0.076 and 0.064 nm, respectively [3]. This finding was evidenced from the observed peaks dislocation.

The dissolution of Al^{3+} ions in the lattices of CoO and Fe_2O_3, involved in the forming cobalt ferrite, can proceed via substitution of some host Co^{2+} and Fe^{3+} ions and/or also by their location in interstitial positions forming solid solution. The dissolution process can be simplified by the use of KrÖger's notations [22] in the following manner:

$$Al_2O_3 \rightarrow 2Al(Co^{2+}) + C.V \quad (2)$$

$$Al_2O_3 \rightarrow Al(Fe^{3+}) + C.V \quad (3)$$

$$Al_2O_3 + 2Co^{2+} \rightarrow 2Al_{\Delta} + 2\,Co^{2+} + C.V \quad (4)$$

$$Al_2O_3 + 2Fe^{3+} \rightarrow 2Al_{\Delta} + 2Fe^{3+} + 2C.V \quad (5)$$

$Al(Co^{2+})$ and $Al(Fe^{3+})$ are the trivalent aluminium ions located in the positions of host cobalt and iron oxides in CoO and Fe_2O_3, respectively; Al_{Δ} is aluminium ions located in the interstitial positions of zinc and ferric oxide lattices; C.V. created cationic vacancies. The dissolution of dopant ions in the lattices of reacting oxides according to the previous reactions (2, 3, 4 and 5) which led to creation of cationic vacancies might increase the mobility of cations of reacting oxides (Co^{2+} and Fe^{3+}) with subsequent an increase in the ferrite formation.

The intensities of the (2 2 0) and (4 4 0) planes are more sensitive to the cations on tetrahedral and octahedral, respectively [3]. Table 1 shows the observed intensities of the above two planes and the intensity ratio between them.

Table 1. The effects of Al- doping on some values of the intensity of (h k l) planes of the as prepared solids.

Dopant concentration (wt%)	Peak height (a. u.)		
	I_{220}	I_{440}	I_{220}/I_{440}
0.0	22.3	41.5	0.537
1.5	32.4	52.6	0.616
3.0	36.8	58.3	0.631

It can be observed that the intensities of the previous planes increase with the addition of aluminium indicating the preference of the Co^{2+}, Fe^{3+} and Al^{3+} ions by the octahedral B and tetrahedral A sites. Indeed, The increase in the intensity of the (2 2 0) plane is greater than that of the (4 4 0) plane. The maximum increase in the intensities of the (2 2 0) and (4 4 0) planes attained of 65 and 40.5 %, respectively. This result might show the increasing amounts of Fe^{3+} located on tetrahedral sites due to alumina doping process. In addition, this may be indicated the solubility of Al_2O_3 at A and B sites on the spinel structure with subsequent redistribution of the cations in the nanostructure cobalt ferrite [3]. This confirms that The Co- ferrite has partially inverted spinel structure. From this data it is evident that the ratio of Fe^{3+}(oct.)/Fe^{3+} (tet.) changes as the Al^{3+} concentration increases. So, it can be suggested that the spinel structure in the prepared materials having the formula $CoAl_xFe_{2-x}O_4$ and can be expressed as:

$$(Co_\delta{}^{2+}\ Al_y\ Fe_{1-\delta}{}^{3+})_A[Co_{\delta-1}{}^{2+}Al_x{}^{3+}\ Fe_{1-x+y+\delta}{}^{3+}]_B\ O_4{}^{2-} \qquad (6)$$

where δ is the parameter of inversion. These observations confirm that the change in the metal ion – oxygen bond distances resulted in a significant modification in the particle size of the investigated ferrites.

An X-ray data enable us to investigation the role of alumina doping in modifying the structural parameters such as the crystallinity (D, the intensity of the (3 1 1) plane), crystallite size (d), lattice constant (a), unit cell volume (V), ionic radii (r_A and r_B), the distance between the magnetic ions (L_A and L_B) and bond lengths (A–O and B–O) on tetrahedral (A) sites and octahedral (B) sites of cubic spinel structure for the produced cobalt ferrite crystallites. The values obtained of various structural parameters are given in Tables 2 and 3.

Table 2. The effects of Al- doping on the values of d, a, V and D of the as prepared solids.

Dopant concentration (wt%)	D (a. u.)	d (nm)	a (nm)	V (nm^3)
0.0	086.1	40	0.848	0.610
1.5	117.7	47	0.844	0.601
3.0	128.9	58	0.840	0.593

Table 3. The effects of alumina doping on the values of L_A, L_B, A-O, B-O, r_A and r_B of cobalt ferrite.

Dopant concentration (wt%)	L_A (nm)	L_B (nm)	A-O (nm)	B-O (nm)	r_A (nm)	r_B (nm)
0.0	0.367	0.300	0.191	0.208	0.056	0.073
1.5	0.365	0.298	0.190	0.207	0.055	0.072
3.0	0.363	0.296	0.189	0.206	0.054	0.071

It can be seen from these tables that the doping with increasing amounts of aluminum oxide brought about a decrease in the values of d, a, V, r_A, r_B, L_A, L_B, A–O and B–O. However, this treatment led to an increase in crystallinity of cobalt ferrite compound. The observed increase in the crystallinity could be attributed to the agglomeration and/or increasing the amount of nano-sized doped cobalt ferrite particles produced depending upon undpoed Co-ferrite is essentially well crystalline particles.

The decrease in the lattice constant and unit cell volume of the as prepared cobalt ferrite maybe due to the difference in the ionic radii of Al, Co and Fe ions. The ionic radii of the Co^{2+}, Fe^{2+} and Fe^{3+} ions are 56, 52 and 28% greater than the Al^{3+} ion [3]. This fact indicates that the doping of our samples with different amounts of alumina resulted in contraction of cobalt ferrite lattices which agglomerated during combustion process. This will confirm by SEM technique. However, the decrease in the values of r_A, r_B, L_A, L_B, A–O and B–O may be explained on the basis of the smaller radii of Al^{3+} ion than that of Fe^{3+} ion, which makes the magnetic ions become closer to each other with subsequent a decrease in the hopping length [23].

3.2. IR analysis

The IR transmission spectra for undoped and alumina doped cobalt ferrite samples were recorded in the range of 1000 - 400 cm^{-1} and are shown in Fig. 2.

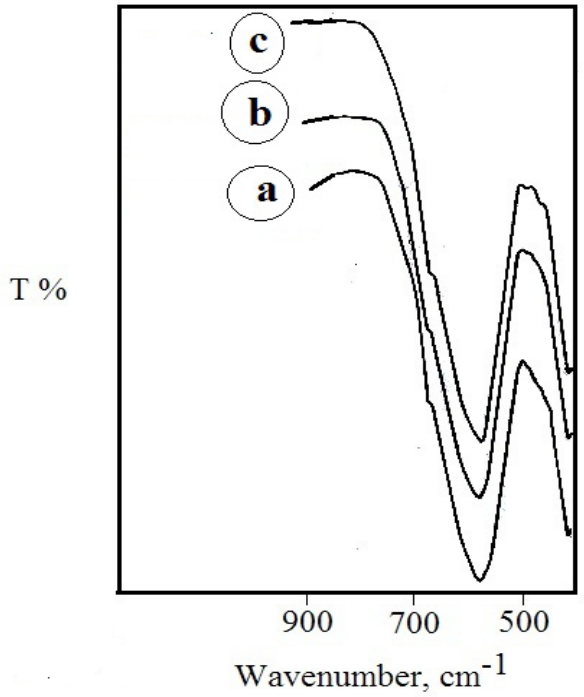

Figure 2. IR spectra of $CoFe_2O_4$ sample treated with different amounts of aluminum oxide; (a) 0 wt% Al_2O_3, (b) 1.5 wt% Al_2O_3 and (c) 3 wt% Al_2O_3.

The frequencies of the vibrations depend on cation oxygen bonding, lattice parameters and cation mass [24]. Ferrites possess the structure of mineral spinel that crystallizes in the cubic form with space group *Fd*3*m* [25]. The spectra of the investigated mixed solids consisted of two main absorption bands at 569±2 (υ_1) and 406±2 cm^{-1} (υ_2). These bands are attributed to the vibration on iron ions in both tetrahedral (A) and octahedral (B) sites of the spinel structure, respectively [26]. In addition, the existence of a weak shoulder (υ_1') at 665 cm^{-1} around the υ_1 band in the IR spectrum of all samples could be attributed to presence of the Co^{2+} ions in tetrahedral site.

3.3. Morphology and microstructure

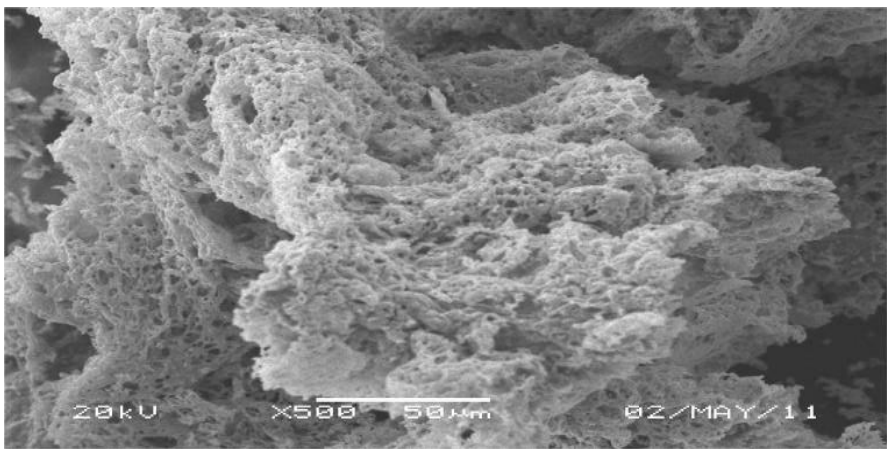

A

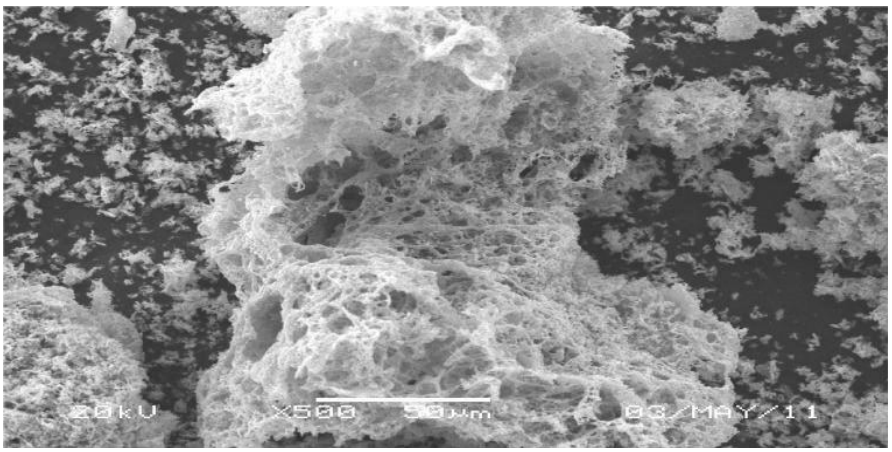

B

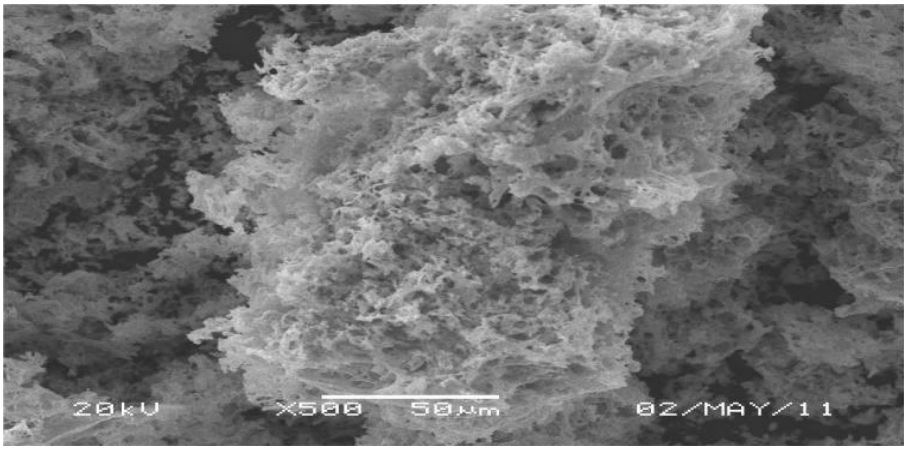

C

Figure 3. SEM images for $CoFe_2O_4$ sample treated with different amounts of aluminum oxide; (a) 0 wt% Al_2O_3, (b) 1.5 wt% Al_2O_3 and (c) 3 wt% Al_2O_3.

The microstructure of undoped and alumina doped cobalt ferrite samples is analyzed using SEM technique. It could be observed that the morphology of the particles is very similar as shown in Fig. 3a - c.

The SEM micrographs show formation of spongy and fragile network structure. Alumina treatment brought about remarkable changes in the microstructure and porosity of the as- prepared zinc ferrite Alumina doping resulted in reduce in the agglomeration process as shown in Fig. 2b and c. In other words, alumina doped cobalt ferrite is less agglomerated than undoped ferrite. However, the surface of the ferrite samples has a number of fine pores or voids which are attributed to the large amount of gases liberated during the combustion process. The presence of a porous network is one of the characteristics of combustion-synthesized powders [27].

This indicates the strong impact of alumina in re-crystallization cobalt ferrite crystals depending upon the redistribution of the cations in both the octahedral and tetrahedral sites involved in the spinel cubic structure. In term of the shape evolution of polyhedral nano-crystals with cubic structures, we can speculate that the ratio of the growth rate along (4 4 0) to that along (2 2 0), played a key role on the morphology of nano-particles [28]. It was believed that during the alumina-doping

followed by the combustion process, the growth rate along (4 4 0) over that along (2 2 0) changed with varied concentrations of alumina. It is interesting to observe some localized fragments as impurities among zinc ferrite nano-particles on the spinel cubic structure. Indeed, the XRD measurements showed that the pattern of 3 wt% Al_2O_3-doped sample consisted of well crystalline single phase of cobalt ferrite. However, these measurements display an increase in the intensity of the (2 2 0) and (4 4 0) planes with the continuous addition of alumina (Table 1) indicating the solubility of Al_2O_3 at A and B sites on the spinel structure with subsequent redistribution of the cations in the nanostructure cobalt ferrite [3].

3.4. Magnetic study

Magnetic hysteresis loops observed for undoped and alumina doped cobalt ferrite system at 300K and applied field of 15 kG are shown in Fig. 4.

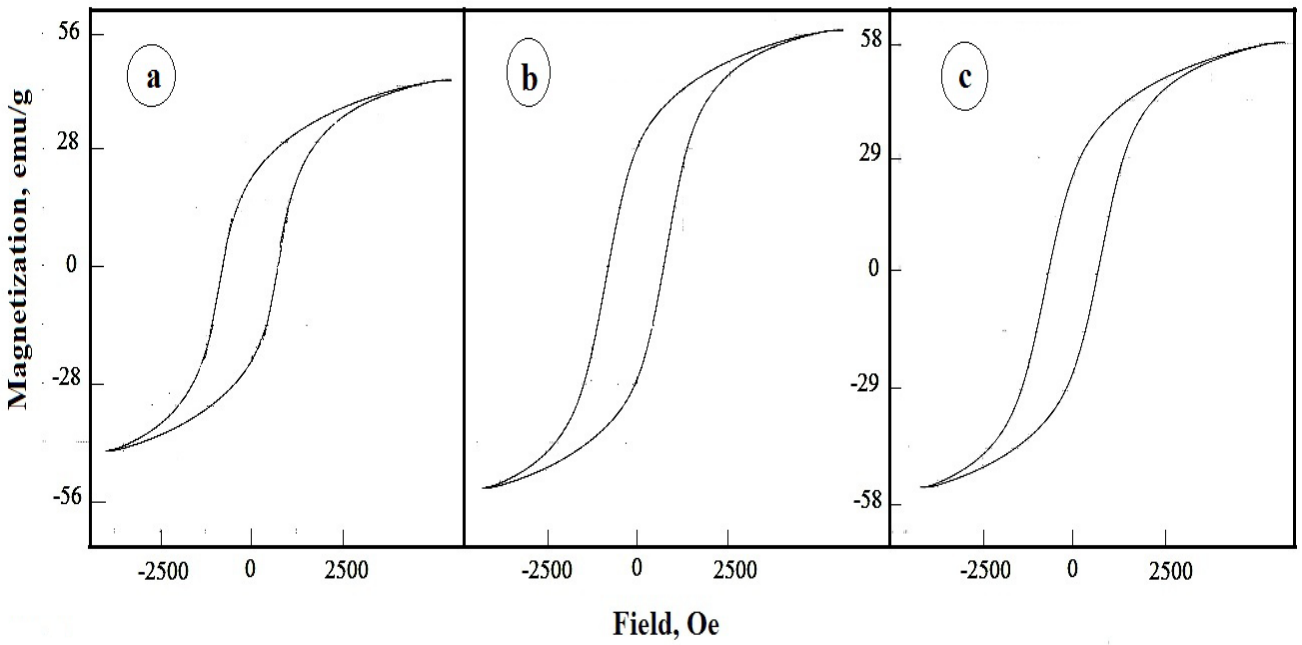

Figure 4. Magnetic hysteresis curves measured at a room temperature for $CoFe_2O_4$ sample treated with different amounts of aluminum oxide; (a) 0 wt% Al_2O_3, (b) 1.5 wt% Al_2O_3 and (c) 3 wt% Al_2O_3.

Most of the samples exhibit moderate magnetization values and small coercive fields in the present work. Similar reports for nano-particles are available in literature [3, 29]. The variation of coercivity, magnetization and magnetic moment (n_B) of the as-prepared ferrite as a function of concentration of alumina is summarized in Table 4.

Table 4. The effects of Al- doping on the magnetic properties (Ms, Mr, Hc and nB) of the as prepared solids.

Dopant concentration (wt%)	Ms (emu/g)	Mr (emu/g)	Mr/Ms (emu/g)	Hc (Oe)	nB
0.0	44.12	19.22	0.455	809	1.85
1.5	56.13	29.60	0.526	764	2.36
3.0	57.28	26.89	0.471	690	2.40

It seen from this table that the maximum increase in both the M_s and n_B values of the $CoFe_2O_4$ crystallite due to the treatment with 3 wt% Al_2O_3 attained 29.8 %. As particle size decreases the occupancy of tetrahedral, A, site by Fe^{3+} ions increases, thereby increasing the interactions between Fe^{3+} ions on A and B sublattices (Fe^{3+}(A)–O–Fe^{3+}(B) interactions) causing high value of magnetic moment [30].

4. CONCLUSIONS

In the present work a novel combustion route is employed for the preparation of undoped and alumina doped cobalt ferrite nano-particles. The results obtained can be summarized as follows:

1- Alumina doping resulted in different modification in the structural properties such as the degree of crystallinity, crystallite size (d), lattice constant (a), unit cell volume (V), ionic radii (r_A and r_B), the distance between the magnetic ions (L_A and L_B) and bond lengths (A–O and B–O) on tetrahedral (A) sites and octahedral (B) sites of cubic spinel cobalt ferrite particles. This treatment led to a decrease in the crystallite size of the investigated system. Opposite behavior was observed for unit cell volume (V), ionic radii (r_A and r_B), the distance between the magnetic ions (L_A and L_B) and bond lengths (A–O and B–O) on tetrahedral (A) sites and octahedral (B) sites of cobalt ferrite crystallites.

2- The proposed cation distributions based on the IR and XRD data show a remarkable difference from the ones reported earlier for bulk particles of similar ferrites. This data showed the evidence for partially inverted cobalt ferrite.

3- Doping of Co/Fe mixed oxides with 3 wt% Al_2O_3 brought about a significant change in the morphology of these oxides with formation of a single phase of $CoAl_xFe_{2-x}O_4$ crystallites.

4- Alumina-treatment mostly resulted in the appearance of the disorder of Co and Fe ions over the A and B-sites, leading to significant variation in the magnetic properties. Indeed, this treatment displays a decrease in the coercivity with an increase in both magnetization and magnetic moment of the investigated ferrite. It has been reported that the magnetic properties of inverted cobalt ferrite arises due to co-existence of Fe^{3+}(A)–O–Fe^{3+}(B) interactions. The propagation in this reaction is controlled by redistribution of Fe^{3+} ions between A and B sites involved in the cubic spinel structure.

ACKNOWLEDGEMENT
The project was supported by the Research Center, College of Science, King Saud University.

References

1. N. M. Deraz, Ph. D. thesis, Investigation of some physicochemical, surface and catalytic properties of some mixed ferrites, Zagazig University, Zagazig, Egypt (1999).
2. N. M. Deraz, *Thermochem. Acta* 401 (2003) 175.
3. N. M. Deraz, *J. Anal. Appl. Pyrolysis* 91 (2011) 48.
4. N. M. Deraz, *J. Anal. Appl. Pyrolysis* 82 (2008) 212.
5. R. Kalai Selvan, C. O. Augustin, L. John Berchmans, R. Saraswathi, *Mat. Res. Bull.* 38(2003)41.
6. Sang Won Lee, Seongtae Bae, Yasushi Takemura, In-Bo Shim, Tae Min Kim, Jeongryul Kim, Hong Jae Lee, Shayne Zurn, Chul Sung Kim, *J. Magn. Magn. Mater.* 310 (2007) 2868.
7. R. Valensuela, Magnetic Ceramics, Cambridge University Press, Cambridge, 1984, p. 191.
8. N. M. Deraz, *J. Anal. Appl. Pyrolysis* 88 (2010) 103.
9. A.R. West, in: Basic Solid State Chemistry, 1998, p. 356.
10. C. Liu, B. Zou, A.J. Rondinone, Z.J. Zhang, *J. Am Chem. Soc.* 122 (2000) 6263.
11. Y. Ahn, E.J. Choi, S. Kim, H.N. Ok, *Mater Lett*. 50 (2001) 47.
12. S.R. Ahmed, P. Kofinas, *Mater. Res. Soc. Symp. Proc.* 661 (2001)KK10.10.1.
13. P.C. Morais, V.K. Garg, A.C. Oliveira, L.P. Silva, R.B. Azevedo, A.M.L. Silva, E.C.D. Lima, *J. Magn. Magn. Mater*. 225 (2001) 37.
14. R.H.G.A. Kiminami, *J. Kona.Powder Part.* 19 (2001) 156.
15. A.C.M. Costa, E. Tortella, M.R. Morelli, M. Kaufman, R.H.G.A. Kiminami, *J. Mater. Sci.* 37 (2002) 3569.
16. S.R. Jain, K.C. Adiga, V.R. Pai Vernecker, *Combust. Flame* 40 (1981) 71.
17. Y. Zhang, G.C. Stangle, *J. Mater. Res*. 9 (1994) 1997.
18. J. L. Dormann, M. Nogues, *J. Phys. Condens. Matter*. 2(1990)1223.
19. Sonal Singhal, S.K. Barthwal, Kailash Chandra, *J. Magn. Magn. Mater.* 306 (2006) 233.
20. K.P. Chae, J. Lee, H.S. Kweon, Y.B. Lee, *J. Magn. Magn. Mater*. 283 (2004) 103.
21. B.D. Cullity, Elements of X-ray Diffraction, Addison-Wesly Publishing Co. Inc. 1976 (Chapter 14).
22. F. A. KrÖger, Chemistry of Imperfect Crystals, North-Holland, Amsterdam, 1964.
23. N. M. Deraz, *J. Alloy Compds* 475 (2009) 832.
24. E.C. Snelling, Soft Ferrites: Properties and Applications, second ed., Butterworth Publishing, London, 1989.
25. D. Ravinder, *Mater. Lett.* 40(1999)205.
26. A. Satter, H. M. El-Sayed, K. M. El-Shokrofy and M. M. El- Tabey, *J. Appl. Sci*. 5 (1) (2005) 162.
27. Yen-Pei Fu, Cheng-Hsiung Lin, Chung-WenLiu, *J. Magn. Magn. Mater.* 283(2004)59.
28. Z. L. Wang, *J. Phys. Chem. B* 104 (2000) 1153.
29. C. Caizer, M. Stefanescu, *Physica B* 327 (2003)129.
30. C. Upadhyay, H. C. Verma, V. Sathe, and A. V. Pimpale, *J. Magn. Magn. Mater.* 312(2007)71.